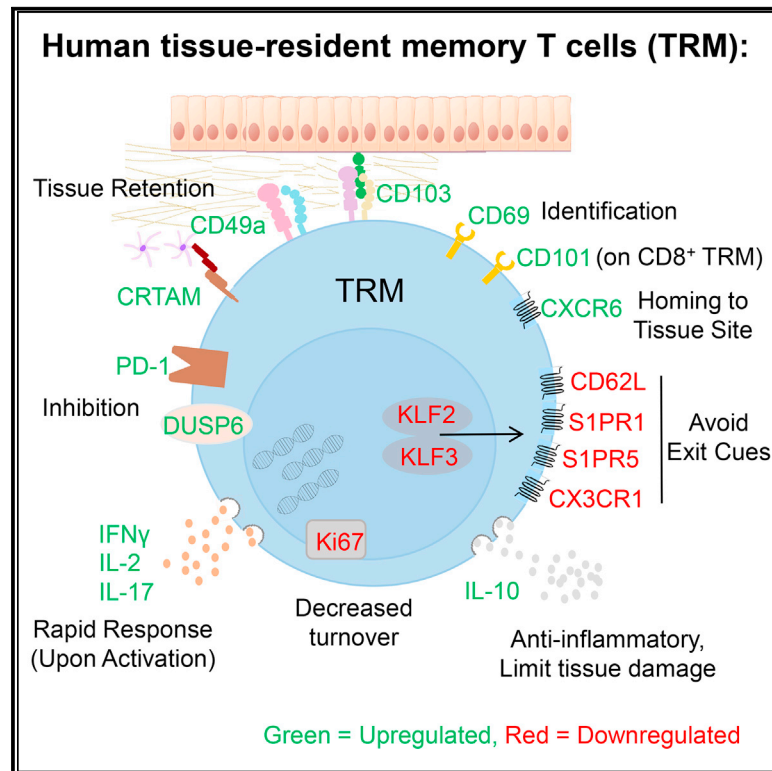


Human Tissue-Resident Memory T Cells Are Defined by Core Transcriptional and Functional Signatures in Lymphoid and Mucosal Sites

Graphical Abstract



Authors

Brahma V. Kumar, Wenji Ma, Michelle Miron, ..., Amy L. Friedman, Yufeng Shen, Donna L. Farber

Correspondence

df2396@cumc.columbia.edu

In Brief

Kumar et al. identify a core transcriptional and phenotypic signature that defines human TRMs for both CD4⁺ and CD8⁺ T cells that is preserved across diverse individuals and in mucosal and lymphoid sites.

Highlights

- CD69⁺ memory T cells predominate in multiple tissues throughout the human body
- A core signature defining human TRMs is enriched within CD69⁺ tissue memory T cells
- Human TRMs have unique adhesion and migratory abilities and functional capacities
- Human TRMs exhibiting the core profile populate multiple lymphoid and mucosal sites

Accession Numbers

GSE94964



Human Tissue-Resident Memory T Cells Are Defined by Core Transcriptional and Functional Signatures in Lymphoid and Mucosal Sites

Brahma V. Kumar,^{1,6} Wenji Ma,^{2,6} Michelle Miron,^{1,3} Tomer Granot,¹ Rebecca S. Guyer,¹ Dustin J. Carpenter,^{1,4} Takashi Senda,¹ Xiaoyun Sun,² Siu-Hong Ho,¹ Harvey Lerner,⁵ Amy L. Friedman,⁵ Yufeng Shen,^{2,7} and Donna L. Farber^{1,3,4,7,8,*}

¹Columbia Center for Translational Immunology, Columbia University Medical Center, New York, NY 10032, USA

²Department of Systems Biology, Columbia University Medical Center, New York, NY 10032, USA

³Department of Microbiology and Immunology, Columbia University Medical Center, New York, NY 10032, USA

⁴Department of Surgery, Columbia University Medical Center, New York, NY 10032, USA

⁵LiveOnNY, New York, NY 10001, USA

⁶These authors contributed equally

⁷Senior author

⁸Lead Contact

*Correspondence: df2396@cumc.columbia.edu

<http://dx.doi.org/10.1016/j.celrep.2017.08.078>

SUMMARY

Tissue-resident memory T cells (TRMs) in mice mediate optimal protective immunity to infection and vaccination, while in humans, the existence and properties of TRMs remain unclear. Here, we use a unique human tissue resource to determine whether human tissue memory T cells constitute a distinct subset in diverse mucosal and lymphoid tissues. We identify a core transcriptional profile within the CD69⁺ subset of memory CD4⁺ and CD8⁺ T cells in lung and spleen that is distinct from that of CD69[−] TEM cells in tissues and circulation and defines human TRMs based on homology to the transcriptional profile of mouse CD8⁺ TRMs. Human TRMs in diverse sites exhibit increased expression of adhesion and inhibitory molecules, produce both pro-inflammatory and regulatory cytokines, and have reduced turnover compared with circulating TEM, suggesting unique adaptations for in situ immunity. Together, our results provide a unifying signature for human TRM and a blueprint for designing tissue-targeted immunotherapies.

INTRODUCTION

The establishment and maintenance of long-term immunity depends on the generation of memory T cells that can populate diverse tissue sites. The effector-memory (TEM) subset (Sallusto et al., 1999) is the predominant subset migrating through multiple tissues (Masopust et al., 2001); however, a significant fraction of TEM-phenotype cells persist as non-circulating subsets of tissue-resident memory T cells (TRMs) in multiple sites, including lungs, intestines, skin, liver, brain, and other mucosal surfaces (for reviews, see Mueller and Mackay, 2016; Schenkel and

Masopust, 2014; Thome and Farber, 2015). TRMs mediate optimal protective responses to site-specific infections through rapid mobilization of immune responses in situ (Schenkel et al., 2014a; Teijaro et al., 2011). Mouse models have also demonstrated the feasibility of targeting TRMs in vaccines for generating protective immunity (Shin and Iwasaki, 2012; Zens et al., 2016). Given their potential importance in immune protection and tissue homeostasis, an understanding of TRM identity, function, and regulation in humans is essential for translating strategies to target tissue-specific responses for protection and immunomodulation.

Advances in human TRM biology are limited by the lack of assays to distinguish circulating and resident memory T cells in tissues. In mice, tissue retention demonstrated by parabiosis (Jiang et al., 2012; Steinert et al., 2015) and in vivo antibody labeling (Anderson et al., 2014; Turner et al., 2014) identified phenotypic markers associated with tissue residence, including CD69 and CD103. In mice, CD69 is expressed by the majority of CD4⁺ and CD8⁺ TRMs in multiple sites (Jiang et al., 2012; Masopust et al., 2006; Schenkel et al., 2013; Teijaro et al., 2011), while CD103 is only expressed by certain subsets of CD8⁺ TRM (Bergsbaken and Bevan, 2015; Mueller and Mackay, 2016) and not significantly by CD4⁺ TRM (Thom et al., 2015; Turner et al., 2014). CD69 has also been shown to have tissue-retention functions in lymph nodes through sequestration of the sphingosine-1-P receptor (S1PR) that mediates egress of T cells (Matloubian et al., 2004; Shioh et al., 2006) and is required for TRM retention in the skin (Mackay et al., 2015). Whether CD69 can delineate TRMs from circulating TEM counterparts remains to be established in humans and is a critical outstanding question in the field.

In human tissues, we and others have identified and characterized TRM phenotype cells expressing CD69 and/or CD103 in multiple sites, including lungs, liver, lymphoid sites, skin, and intestines (Hombrink et al., 2016; Pallett et al., 2017; Purwar et al., 2011; Sathaliyawala et al., 2013; Thome and Farber, 2015; Thome et al., 2014; Watanabe et al., 2015; Wong et al.,



2016; Woon et al., 2016). However, it is not known whether TRMs represent a distinct subset in humans for both CD8⁺ and CD4⁺ T cell lineages, with unifying functional, phenotypic, and transcriptional signatures across tissues and individuals.

We have established a human tissue resource to obtain blood and multiple lymphoid and mucosal tissues from previously healthy organ donors, enabling analysis of T cell compartmentalization and maintenance throughout life (Gordon et al., 2017; Sathaliyawala et al., 2013; Thome et al., 2014, 2016a, 2016b). We present here transcriptional, phenotypic, and functional analyses that define human TRMs as a distinct subset in multiple sites. We show that CD69 is a key marker that distinguishes memory T cells in tissues from those in circulation, while CD103 is expressed only by a subset of tissue memory CD8⁺ and not by CD4⁺ T cells. CD69⁺ tissue memory T cells are transcriptionally and phenotypically distinct from CD69[−] memory T cells in tissues and blood and exhibit a core gene profile comprising adhesion, migration, and regulatory molecules with homology to mouse TRMs. This core signature is shared between human CD4⁺ and CD8⁺ TRM and in multiple lymphoid and mucosal tissues. Further, human TRMs have an enhanced capacity for production of certain cytokines and regulatory molecules and decreased turnover compared to circulating TEM cells, suggesting long-term maintenance in situ. Together, our study establishes human TRMs as a distinct subset stably maintained in diverse anatomic locations.

RESULTS

CD69⁺ Memory Populations Exist Only in Tissues and Do Not Show Evidence of Activation

To identify the major phenotypic marker distinguishing tissue from circulating memory T cells, we assessed CD69 and CD103 expression as markers associated with TRMs in mice by CD45RA[−]/CCR7[−] TEM-phenotype CD4⁺ and CD8⁺ T cells in blood and 8 tissue sites of individual donors (Figures 1A and 1B). We focused on TEM cells as the major memory subset in tissues that is common to both CD4⁺ and CD8⁺ T cells as previously determined (Thome et al., 2014). While blood memory T cells were predominantly CD69[−]/CD103[−], the majority (>50%–90%) of tissue memory CD4⁺ and CD8⁺ T cells in all sites examined—including lungs, intestines, salivary glands, tonsils, spleen, and various lymph nodes (LNs)—expressed CD69 (Figures 1A and 1B). CD103 was expressed predominantly by memory CD8⁺ T cells in tissues associated with the oral-gastrointestinal tract (salivary glands, tonsils, and intestines) and lung, with significantly lower proportions of CD103⁺CD8⁺ memory T cells in spleen and lymph nodes (10%–30%), with few tissue memory CD4⁺ T cells expressing CD103 (<5%–10%; Figures 1A and 1B). Together, these findings indicate that CD69 expression distinguishes tissue from blood TEM across multiple lymphoid and barrier tissues and CD4/CD8 lineages, while CD103 expression is more variable and confined to certain tissue CD8⁺ T cells.

Because CD69 is also a marker of early activation, we assessed the expression of the activation markers CD25, CD38, and HLA-DR by CD69⁺ and CD69[−] memory subsets

from representative lymphoid (spleen) and mucosal (lung) tissues. There was uniformly low expression of CD25, CD38, and HLA-DR on CD69⁺ TEM cells similar to expression levels on resting naive T cells (Figure 1C). Previously, we also found maintenance of CD28 and CD127 expression by the majority of CD69⁺ tissue memory T cells, indicative of a quiescent state (Thome et al., 2014). Together, our results show that CD69 expression by tissue memory T cells is not associated with markers of recent activation.

Human CD69⁺ Tissue Memory T Cells Constitute a Transcriptionally Distinct Subset with Features of Tissue Residency

Based on the aforementioned phenotype analysis, we hypothesized that human TRMs could be found within the CD69⁺ subset of tissue memory T cells. We isolated CD4⁺ and CD8⁺ TEM cells from the spleen and lungs of 3 previously healthy organ donors (sorting strategy is shown in Figure 1D; donor information is shown in Table S1), fractionated them into CD69⁺ and CD69[−] subpopulations for whole-transcriptome profiling by RNA sequencing (RNA-seq), and analyzed the resultant profiles of CD69⁺ and CD69[−] subsets for each lineage and tissue. Principal-component analysis (PCA) revealed that the transcriptome of CD69⁺ cells was distinct from that of the CD69[−] subset for CD4⁺ and CD8⁺ memory T cells in spleen and lung tissue for all three donors analyzed (Figure 2A). This result indicates that CD69 expression defines a transcriptionally distinct subset of memory T cells in human tissues.

Applying the criteria for significance (false discovery rate [FDR] ≤ 0.05, and absolute value of log₂ fold change ≥ 1), for CD4⁺ samples, we identified 327 genes differentially expressed between lung CD69⁺ and CD69[−] subsets and 221 genes differentially expressed between spleen CD69⁺ and CD69[−] subsets, of which 77 genes (29 upregulated, 48 downregulated) were differentially expressed in both tissues (Figures 2B and 2C). For CD8⁺ samples, we identified 329 genes differentially expressed between lung CD69⁺ and CD69[−] subsets and 459 genes differentially expressed between spleen CD69⁺ and CD69[−] subsets, of which 133 genes (39 upregulated, 94 downregulated) were differentially expressed in both tissues (Figures 2B and 2C). The expression differences in these key genes were similar between three donors (Figure 2C).

The genes differentially expressed by human CD69⁺ and CD69[−] TEM cells (Figure 2C) included key molecules associated with mouse CD8⁺ TRMs from infection models (Mackay et al., 2013, 2016; Skon et al., 2013; Wakim et al., 2012). Notably, downregulation of S1PR1 and its associated transcription factor KLF2 are required for CD8⁺ TRM establishment in mice (Skon et al., 2013), and we found striking downregulation of S1PR1 (8- to 16-fold) and KLF2 (2- to 16-fold) transcripts for all CD69⁺ subsets compared with CD69[−] subsets in every donor for both CD4⁺ and CD8⁺ T cells in lung and spleen (Figure 2D). In addition, human CD8⁺CD69⁺ subsets exhibited upregulation of ITGAE (CD103), ITGA1 (CD49a), ICOS, and the transcription factor IRF4, which was also found to be upregulated by mouse CD8⁺ TRMs in different systems (Mackay and Kallies, 2017). Together, these results show that the CD69⁺ tissue memory T cells constitute a

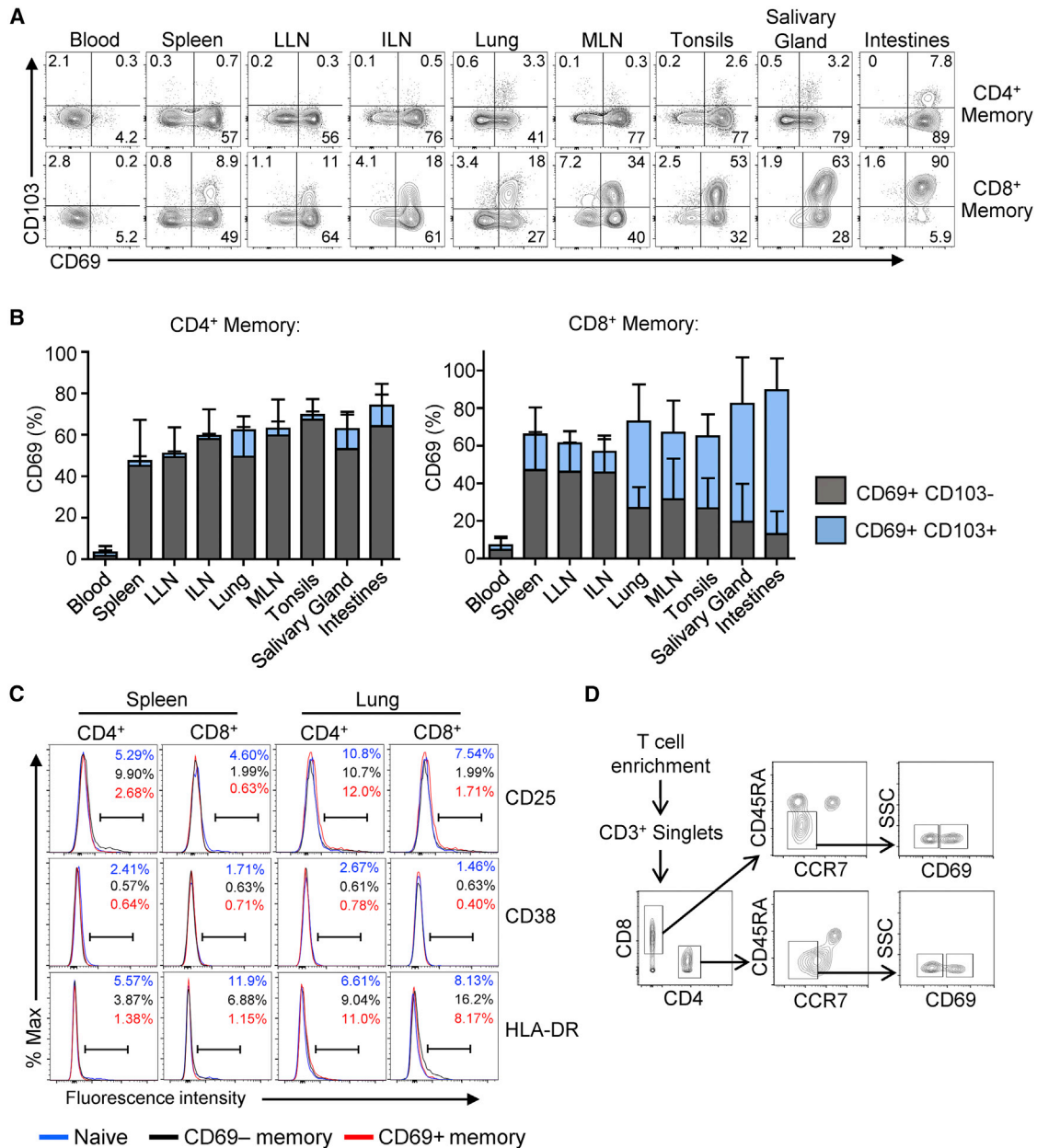


Figure 1. CD69+ Memory T Cells Are Prevalent in Tissues and Do Not Show Features of Activation

(A) Expression of CD69 and CD103 by CD4⁺ (top) and CD8⁺ (lower) memory T cells (CCR7⁺ CD45RA⁺) within each indicated site from one individual (donor 332) representative of 6 donors. LLN, Lung lymph node; ILN, inguinal lymph node; MLN, mesenteric lymph node.

(B) Mean frequency (\pm SEM) of CD69⁺CD103⁻ (gray) and CD69⁺CD103⁺ (blue) CD4⁺ (left) and CD8⁺ (right) memory T cells in each tissue compiled from 16–22 donors per site.

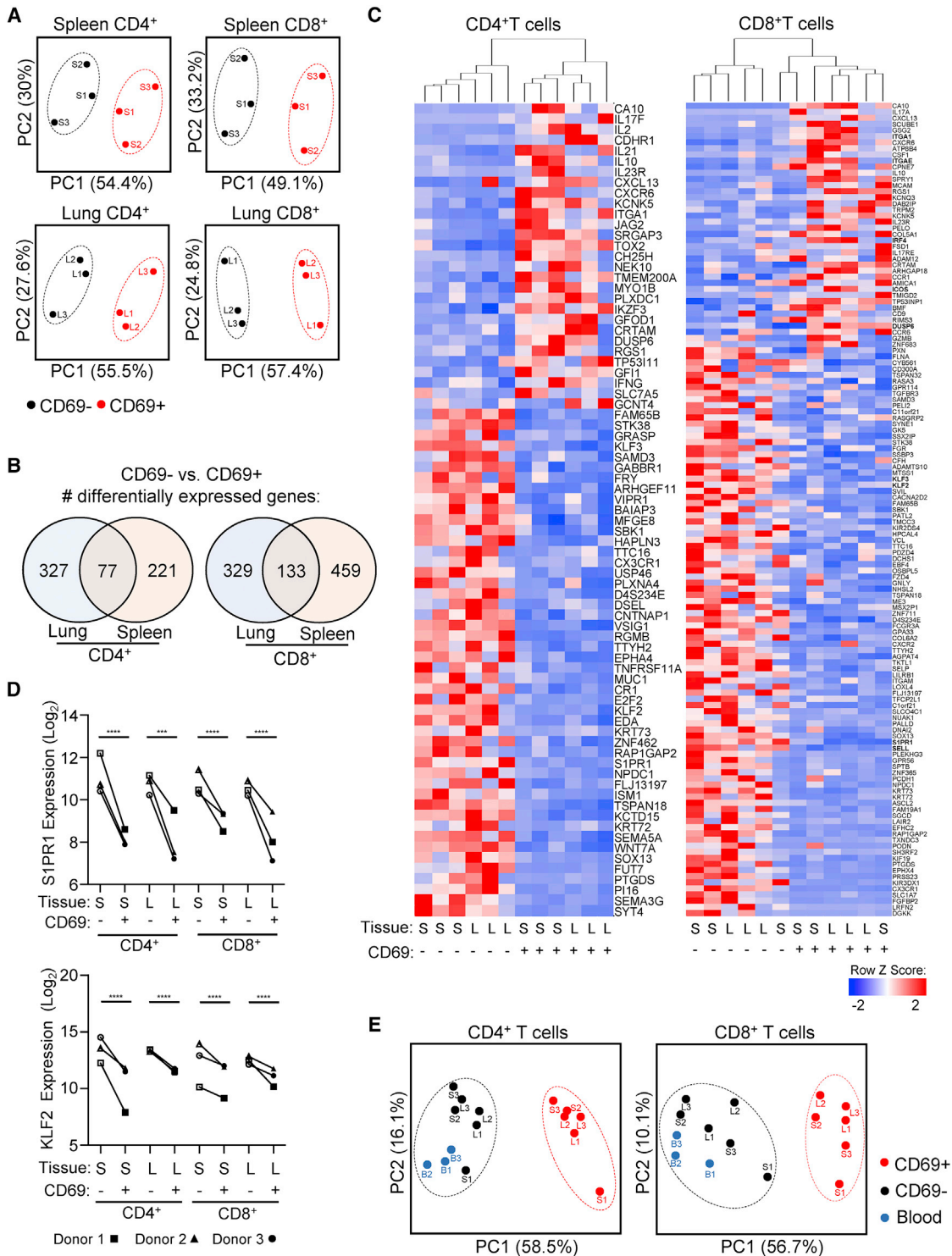
(C) Activation profile of T cells from human tissues. Flow cytometry plots show expression of CD25, CD38, and HLA-DR by naive T cells (CCR7⁺ CD45RA⁺, blue line), and CD69⁻ (black) and CD69⁺ (red) subsets of memory T cells (CCR7⁺ CD45RA⁺). Data are representative of 3 donors.

(D) Sorting strategy for isolation of CD4⁺ and CD8⁺ CD45RA⁻ CCR7⁻ CD69⁺ and CD45RA⁻ CCR7⁻ CD69⁻ T cells for RNA-seq is shown from spleen.

transcriptionally distinct subset enriched for features of tissue residency.

We further compared the transcriptional profiles of tissue memory T cell subsets with circulating TEM cells isolated from the blood of three healthy volunteers. PCA using the gene signature in Figure 2C resulted in clustering of blood TEM with CD69⁻

tissue TEM, distinct from CD69⁺ samples, which clustered together (Figure 2E). By contrast, PCA using an equal number of randomly selected genes as a negative control yielded no clustering pattern (Figure S1). This grouping suggests that CD69 expression by memory T cells in tissues distinguishes circulating memory subsets from those retained in tissues.



A Core Gene Signature of Human CD69⁺ Memory T Cells

Based on the gene expression analysis in Figure 2, we identified 31 core genes with consistent significant differential expression by CD4⁺ and CD8⁺ CD69⁺ compared with the corresponding CD69[−] subset from lung, spleen, and blood (Figure 3A; Table S2). This core signature included upregulation of the adhesion markers ITGAE (CD103) and ITGA1 (CD49a); the chemokine receptors CXCR6 and CX3CR1; and molecules with known inhibitory functions in T cells, including PDCD1 (PD-1) (Barber et al., 2006), the dual-specificity phosphatase DUSP6 that turns off MAP kinase signaling (Bertin et al., 2015), and interleukin (IL)-10. Downregulated genes within the core signature included S1PR1 and its associated transcription factor KLF2, which together control T cell homing and tissue retention (Skon et al., 2013); the related Kruppel-like transcription factor KLF3; and the lymph node homing receptor SELL (CD62L); as well as RAP1GAP1 and RGS1, G-protein-signaling genes that modulate T cell trafficking (Gibbons et al., 2011).

Pathways represented within the core signature include those controlling T cell adhesion and migration, proliferation, development, and activation (Table S3) that interconnect as diagrammed in Figure 3B. Many of the upregulated genes map downstream of T cell receptor (TCR) signaling, including CD69, adhesion molecules (ITGA1, ITGAE, and CRTAM), and activation-induced molecules IL-2, IL-10, and PD-1 that can regulate proliferation (Figure 3B). Differential upregulation or downregulation of specific chemokines and chemokine receptors (CXCL13, CXCR6, CX3CR1, SELL, and S1PR1) and modulation of G-protein-mediated signaling (Figure 2B) indicate that tissue residence involves specific tuning of migratory properties. Overall, these results establish that human CD69⁺ tissue memory T cells maintain a core signature impinging on multiple signaling pathways affecting cellular migration, function, and proliferation.

The relative transcript levels of key genes within the core gene signature (ITGA1 [CD49a], CXCR6, ITGAE [CD103], CXCR6, CX3CR1, and PD-1) showed differential regulation between CD69⁺ and CD69[−] subsets that was consistent across tissues, lineages, and diverse donors (Figures 3C–3G). We also validated differential surface protein expression for each marker compiled from 8 to 20 donors (Figures S2 and S3; discussed later). Interestingly, for a number of genes (ITGAE, CX3CR1, and PDCD1), there was an expression gradient from blood to tissue CD69[−] to CD69⁺ subsets, with blood memory cells exhibiting lower (ITGAE and PDCD1) or higher (CX3CR1) expression than CD69[−] subsets from tissues (Figures 3D, 3F, and 3G), suggesting some differences between CD69[−] subsets in blood and tissues. Together, these data establish CD49a, CD103, CXCR6, CX3CR1, and PD-1 as core surface markers that distinguish

human CD69⁺ and CD69[−] memory subsets across tissues and lineages.

The Human CD69⁺ Tissue Memory Core Signature Bears Key Homologies with Mouse TRMs

To determine whether the core transcriptional profile common to CD69⁺ memory T cells in spleen and lungs defined a TRM signature, we compared the RNA-seq profile of the human tissue and blood subsets with that of mouse antigen-specific CD8⁺ TRMs isolated from skin and intestines following infection (Mackay et al., 2016). PCA of whole transcriptomes shows species-specific transcriptional differences between human and mouse T cells dominating, with all human samples clustering together distinct from mouse TRM/TEM, and mouse samples forming distinct clusters based on the infection model (Figure 4A, left). When analyzed based on the human core gene signature in Figure 3, CD4⁺CD69⁺ and CD8⁺CD69⁺ subsets from human spleen and lung cluster together with mouse CD8⁺ TRMs from skin and gut in the two different infection models and are distinct from all TEM/CD69[−] counterparts (Figure 4A, right). Gene set enrichment analysis (GSEA) (Subramanian et al., 2005) also revealed a strong enrichment of the differentially expressed genes in human CD4⁺CD69⁺ and CD8⁺CD69⁺ subsets within the gene signatures of TRMs from mouse brain (Wakim et al., 2012) and from mouse skin and lung (Mackay et al., 2013) (Figure 4B). Taken together, our results show that the gene signature of human CD69⁺ tissue memory T cells exhibits key features of TRMs and likely contain the human TRM subset.

A recent report showed that mouse CD8⁺ TRM in multiple tissues exhibit biased expression of the Hobit (homolog-of BLIMP in T cells) transcription factor, which can drive TRM differentiation in vivo (Mackay et al., 2016). As Hobit was not part of the core gene set in our analysis, we specifically analyzed the expression level of Hobit (ZNF683) by human CD69⁺ memory T cells compared with mouse TRMs. In mouse TRMs, Hobit levels were higher than the housekeeping gene GAPDH and comparable to CD69 transcript levels. By contrast, for human CD69⁺ memory T cells, Hobit transcript levels were below median gene expression and significantly lower than GAPDH and CD69 levels (Figure 4C). These results suggest distinct molecular control of human and mouse TRM differentiation, despite similar core signatures.

Reduced Clonal Overlap and Proliferative Turnover of CD69⁺ Compared with CD69[−] Memory T Cells

We compared the TCR repertoires of lung and spleen CD69⁺ and CD69[−] memory T cell subsets using a recently developed algorithm TRUST (TCR Repertoire Utilities for Solid Tissue) (Li et al.,

(B) Diagram shows the number of significant differentially expressed genes ($FDR \leq 0.05$, and \log_2 fold change ≥ 1) between CD69[−] and CD69⁺ samples within each tissue for CD4⁺ and CD8⁺ T cells showing overlap between tissues.

(C) Heatmap showing normalized expression levels of the overlap genes identified in (B) for CD4⁺ (77 genes) and CD8⁺ (133 genes) CD69[−] versus CD69⁺ subsets from spleen (S) and lung (L).

(D) Transcriptional downregulation of S1PR1 and KLF2 in all CD69⁺ subsets versus CD69[−] subsets. Normalized expression levels of S1PR1 (top) and KLF2 (bottom) transcripts in CD69[−] and CD69⁺ samples from spleen (S) and lung (L) of each donor are shown. Individual donors are indicated by distinct symbols, and lines connect samples from identical donors within a tissue. *** $FDR \leq 10^{-3}$; **** $FDR \leq 10^{-5}$.

(E) PCA of CD69⁺ (red) and CD69[−] (black indicates tissue; blue indicates blood) memory subsets based on the genes in (C). S, spleen; L, lung; B, blood. See also Figure S1 and Table S6.

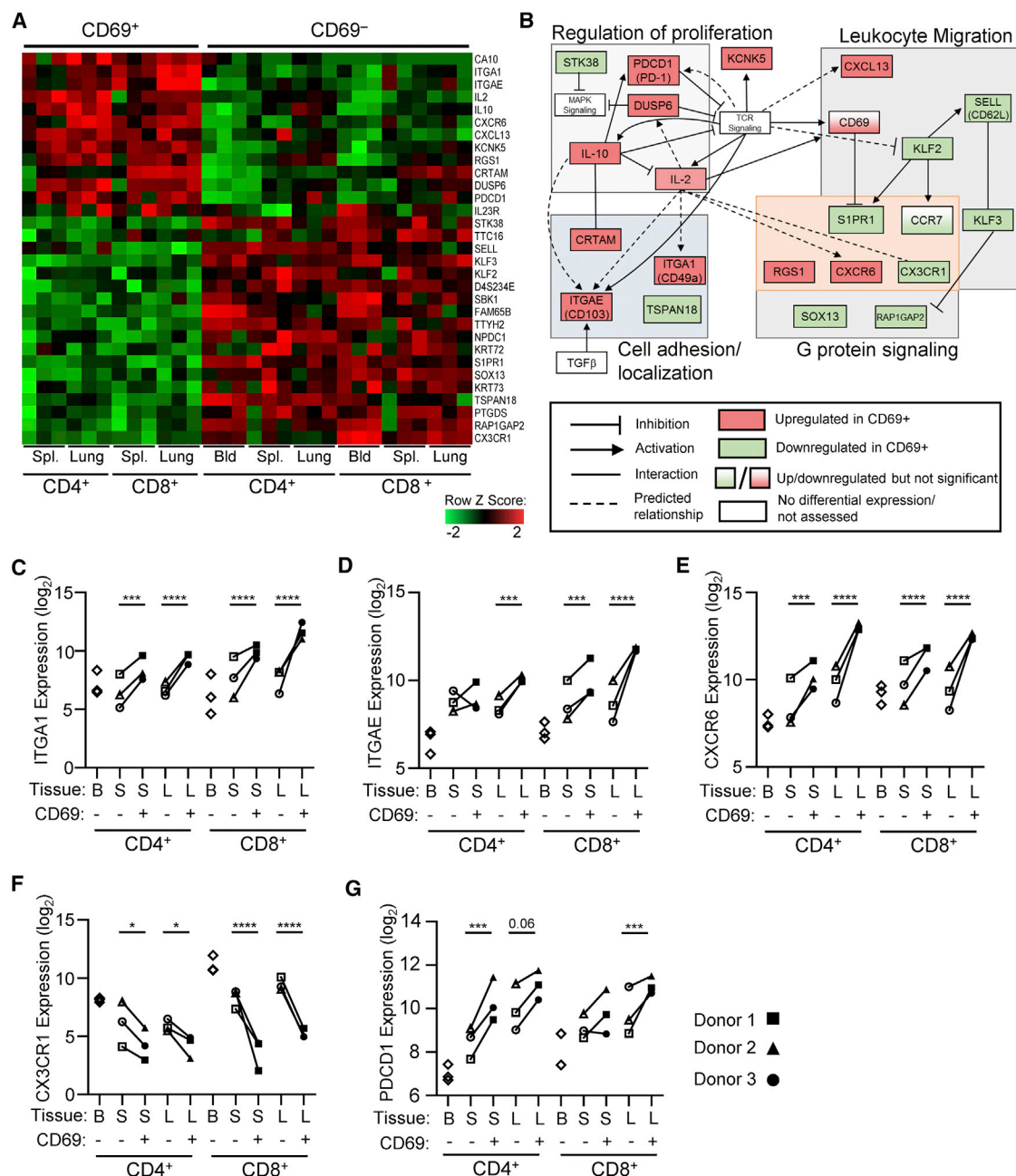


Figure 3. A Core Gene Signature Defines Tissue CD69⁺ Memory T Cells Distinct from Circulating CD69⁻ Cells in Tissues and Blood

(A) Heatmap shows normalized expression of genes with significant differential expression between CD69⁺ and CD69⁻ memory T cells for all subsets (CD4⁺ and CD8⁺) and tissues (spleen and lung).

(B) Network analysis of the core gene set in (A) showing known and predicted interactions (activating, inhibitory) between proteins encoded by the core genes that are upregulated (red) or downregulated (green) by TRMs compared with TEM, with key pathways indicated in the shaded boxes. Relationships were determined using IPA software, the STRING protein database, GeneCards, and PubMed literature searches.

(C–G) Normalized mRNA expression levels of ITGA1 (C), ITGAE (D), CXCR6 (E), CX3CR1 (F), and PDCD1 (G) by CD4⁺ and CD8⁺ CD69⁺ and CD69⁻ memory subsets in blood (B), spleen (S), and lung (L) of each individual donor. *FDR ≤ 0.05; ** FDR ≤ 10⁻²; ***FDR ≤ 10⁻³; and ****FDR ≤ 10⁻⁵. Each donor is represented by a unique shape as indicated.

See also [Figures S2](#) and [S3](#).

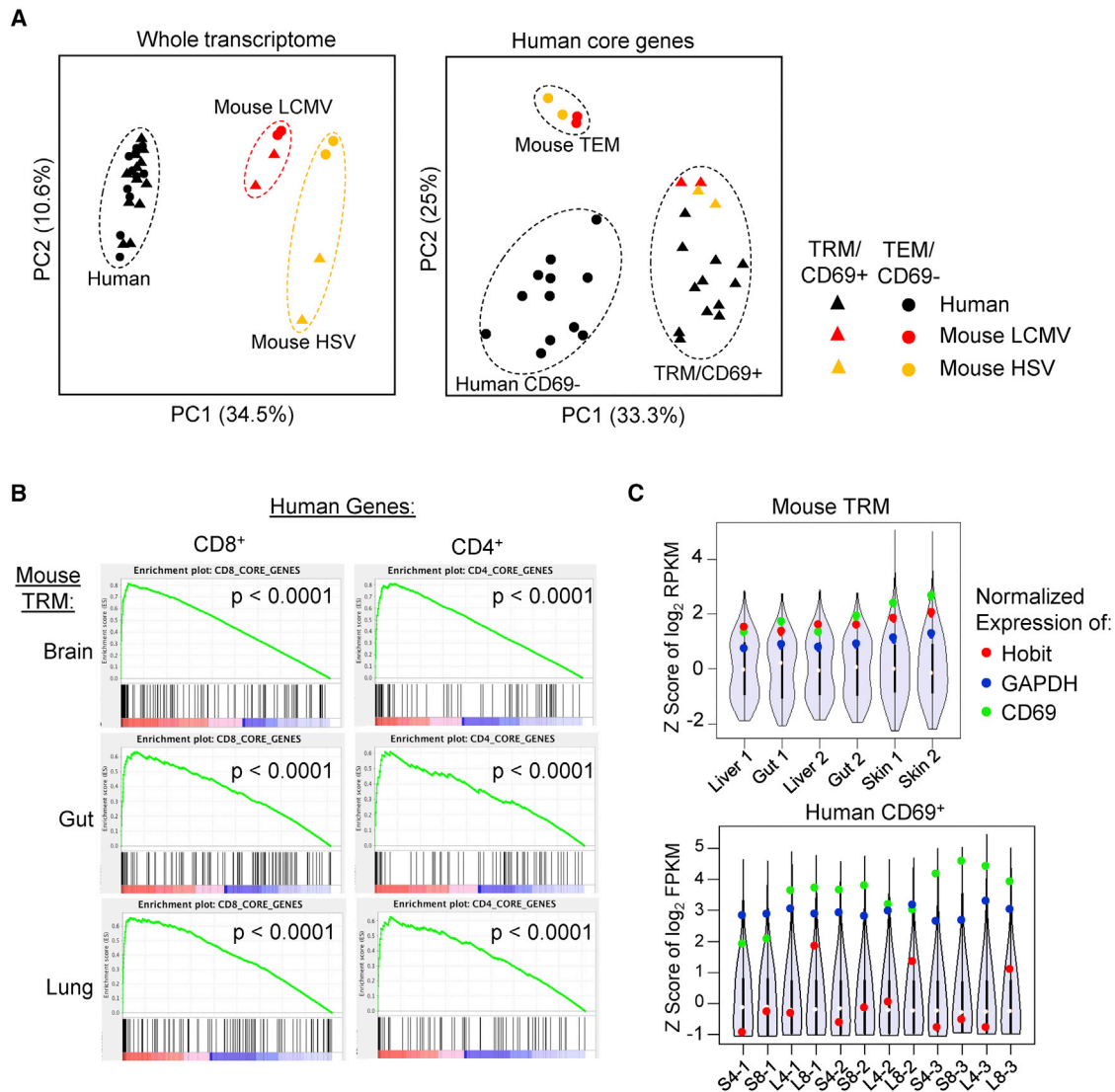


Figure 4. Comparison of the Human and Mouse TRM Transcriptome

(A) PCA was performed using RNA-seq data presented here (black symbols) compared to mouse herpes simplex virus (HSV)-specific CD8⁺ TRMs from skin and CD8⁺ TEM from spleen ("Mouse HSV," yellow) and LCMV-specific CD8⁺ TRMs from intestine and CD8⁺ TEM from spleen ("Mouse LCMV," red) (Mackay et al., 2016). Left: PCA comparing whole transcriptomes of each dataset comprising 15,571 common genes between human and mouse. Right: PCA comparing human and mouse datasets using the core human signature of 31 genes (Figure 3).

(B) Gene set enrichment analysis (GSEA) comparing our human CD8⁺ (left) and CD4⁺ (left) gene sets to published microarray data of CD103⁺ brain TRMs versus spleen TEM (top row), gut TRMs versus spleen TEM (middle row), and lung TRMs versus spleen TEM (bottom row) (Wakim et al., 2012; Mackay et al., 2013). In each plot, the x axis shows the genes ranked with absolute value of log fold change between TRMs versus TEM, and the y axis shows the running enrichment score (ES), comparing the ranked list of genes with indicated p values.

(C) Comparison of Hobit gene expression in mouse and human datasets. Violin plots show the Z score of gene expression levels from mouse TRMs (from Mackay et al., 2016) and human CD69⁺ memory T cells (this study). Red dots represent Hobit, blue dots represent the housekeeping gene GAPDH, green dots represent CD69, and the white dot represents median gene expression.

2017) to extract TCR sequences from the RNA-seq reads (Supplemental Experimental Procedures). Between 0.1% and 0.3% of mapped reads could be assigned to the TCR region (data not shown), with detection of several hundred to over 1,000 unique clonotypes per sample (Figure S4). From these data, we measured clonal diversity (number of unique clonotypes per TCR-mapped reads) and overlap between sites. Overall, CD69⁺

and CD69⁺ cells exhibited similar clonal diversity with CD4⁺ subsets maintaining higher clonal diversity compared to CD8⁺ memory subsets (Figure 5A), consistent with our previous findings showing increased clonality of memory CD8⁺ compared to CD4⁺ T cells from lymphoid sites (Thome et al., 2014). Clonal overlap between sites was minimal (<1%) for CD4⁺ subsets, while CD8⁺CD69⁺ cells exhibited significantly reduced overlap between

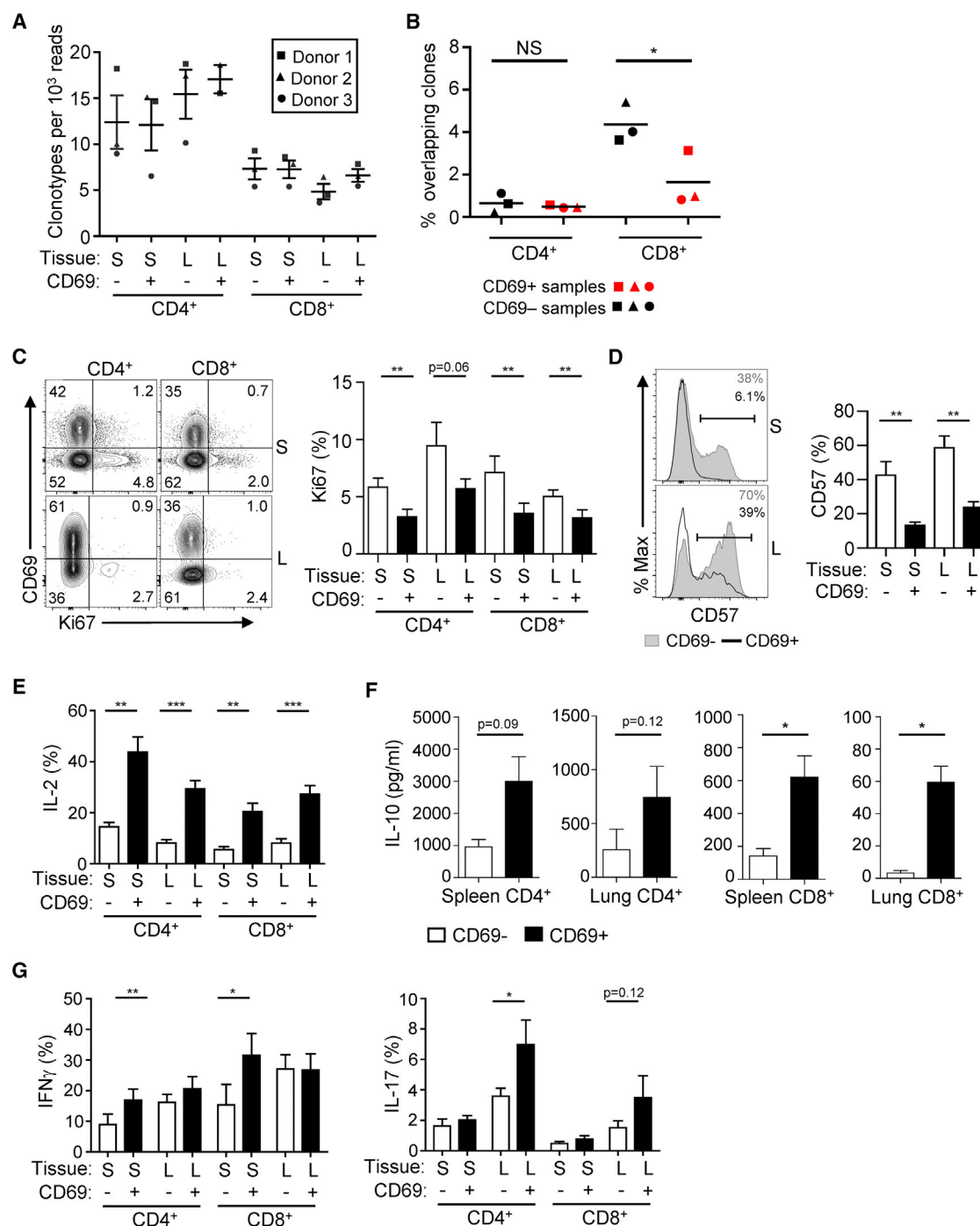


Figure 5. TCR Clonal Analysis, Turnover, and Function of CD69⁺ and CD69⁻ Cells

(A) CD8⁺ T cells have reduced TCR repertoire diversity compared with CD4⁺ cells. CDR3 sequences were inferred from RNA-seq data using TRUST (Supplemental Experimental Procedures). Graph shows the number of unique CDR3 calls (clonotypes) in each sample per 10^3 reads mapped to the TCR region. (B) Increased tissue overlap of TCR clones within CD8⁺ CD69⁻ compared to CD69⁺ memory T cells. Graph shows percentage of overlapping clones between lung and spleen samples from each donor, calculated by dividing the total number of overlapping clones by the total number of unique clones present in both tissues. (C) Reduced proliferative turnover by CD69⁺ memory T cells. Left: representative flow cytometry plots of intracellular Ki67 expression from spleen and lungs of one individual donor. Right: Ki67 expression compiled from 10 donors indicated as mean frequency Ki67⁺ \pm SEM. (D) Increased CD57 expression by CD69⁻ compared to CD69⁺ cells. Left: CD57 expression by CD69⁻ and CD69⁺ memory T cell subsets from spleen and lung of one representative donor. Right: CD57 expression compiled from 11 donors indicated as mean percent positive \pm SEM. *p \leq 0.05; **p \leq 0.01.

(legend continued on next page)

lung and spleen compared to CD8⁺CD69[−] cells (Figure 5B), indicating that CD69⁺ memory T cells are more clonally segregated within the tissue compared to CD69[−] cells. These results provide some additional evidence that CD69⁺ memory T cells may be more retained in the tissue site compared with CD69[−] cells.

We hypothesized that the biased maintenance of CD69⁺ clones in certain sites may indicate reduced turnover. The frequency of CD69⁺ cells expressing Ki67, a marker of proliferating cells, was markedly reduced relative to CD69[−] cells in both spleen and lung (Figure 5C). Examination of CD57 expression, a marker of replicative senescence and terminal differentiation (Kared et al., 2016), revealed lower CD57 expression by CD8⁺CD69⁺ cells compared to CD8⁺CD69[−] cells in both spleen and lung. Taken together, these data suggest that human CD69⁺ memory T cells undergo reduced proliferative turnover and have reduced clonal overlap compared with CD69[−] cells.

Human CD69⁺ Memory T Cells Have a Distinct Functional Profile

We investigated cytokine production by CD69⁺ and CD69[−] cells based on differential transcript expression of genes encoding IL-2, interferon (IFN)- γ , IL-17, and IL-10, identified as significantly upregulated by CD69⁺ versus CD69[−] memory T cells for the CD4⁺ and/or CD8⁺ subsets (Figures 2C and 3A). IL-2 and IL-10 were produced by a consistently higher proportion of CD69⁺ compared with CD69[−] memory T cells for both CD4⁺ and CD8⁺ subsets in spleen and lung (Figures 5E and 5F), consistent with increased IL2 and IL-10 transcription being part of the core signature (Figure 3A). IFN- γ was produced by spleen and lung memory CD4⁺ and CD8⁺ T cells, with spleen CD69⁺ memory T cells exhibiting increased IFN- γ production compared with CD69[−] cells, while lung CD69⁺ and CD69[−] cells had comparable IFN- γ production (Figure 5G, left). IL-17 was produced more extensively by lung CD4⁺ and CD8⁺CD69⁺ compared with lung CD69[−] memory T cells, and not significantly by spleen CD69⁺ and CD69[−] cells (Figure 5G, right). Together these results indicate that the functional capacity of CD69⁺ memory T cells comprises core features (e.g., IL-2 and IL-10 production) along with subset and tissue influences.

The TRM Transcriptional Profile Is Conserved across Lineages and Tissues

Isolation of both CD4⁺ and CD8⁺ memory T cell subsets from two tissue sites of individual donors enabled us to assess lineage- and tissue-specific gene expression patterns. To identify lineage-specific genes, we compared differential gene expression by CD8⁺CD69⁺ versus CD69[−] and CD4⁺CD69⁺ versus CD69[−] subsets for each tissue site. The majority of genes showed similar differential expression in terms of direction and magnitude of fold

change when looking at CD69⁺ versus CD69[−] subsets from either CD8⁺ or CD4⁺ lineages (Figure 6A). From a total of 907 genes that were differentially expressed by at least one of our CD69⁺ versus CD69[−] pairs, there were 4 protein-coding genes that showed differential expression in CD4⁺, but not in CD8⁺, subsets and 27 genes that showed significant differential expression in CD8⁺, but not in CD4⁺, subsets (Figures 6A, S5A, and S5B). Together, these results indicate that the differential expression profile of human CD69⁺ tissue memory T cells is similar across CD4⁺ and CD8⁺ lineages.

We applied a similar type of analysis as in Figure 6A to identify genes specific to lung or spleen memory T cells (Figure 6B). Only 10 genes showed differential expression in CD69⁺ versus CD69[−] in lung, but not spleen, samples and 12 genes that showed significant differential expression in CD69⁺ versus CD69[−] in spleen, but not lung, samples (Figures 6B, S5C, and S5D). Notably, CD101, encoding a cell-surface immunoglobulin superfamily protein that inhibits T cell activation and proliferation (Soares et al., 1998), was transcriptionally upregulated in lung, compared to spleen, memory T cells. However, examination of CD101 surface expression by flow cytometry revealed increased expression by CD8⁺CD69⁺ compared with CD69[−] cells in both lung and spleen, with minimal upregulation by CD4⁺ tissue memory subsets (Figure 6C). These results indicate that CD101 could be an additional marker for CD8⁺ TRMs.

TRMs Are a Phenotypically Distinct Subset across Multiple Tissues

We asked whether multiple elements within the core signature together distinguished tissue memory subsets in spleen and lung using t-distributed scholastic neighbor embedding (t-SNE) analysis (van der Matten and Hinton, 2008; Wong et al., 2016), a dimensionality reduction method used to visualize high-dimensional data in two dimensions so that cells expressing similar markers will be close to each other. Based on the expression of 6 markers defined as part of the core TRM signature (Figure 3)—CD49a, CD103, CXCR6, CX3CR1, PD-1, and CD101—we found that CD69⁺ and CD69[−] subsets were located in distinct regions of the t-SNE plots for both CD4⁺ and CD8⁺ T cells in each tissue (Figure 7A) and in density plots compiled from both sites (Figure 7B, top). Manual gating within each dominant cluster revealed that CD69[−] subsets exhibit elevated expression of CX3CR1 and low expression of CD49a, PD-1, CD101, and CXCR6 compared to CD4⁺ and CD8⁺CD69⁺ subsets exhibiting high expression of CD49a, PD-1, and CXCR6 and low expression of CX3CR1, with CD8⁺CD69⁺ subsets having coordinate expression of CD103 and CD101 (Figure 7B). These results further support the designation of tissue CD69⁺ memory T cells as TRMs and the CD69[−] subset as TEM.

(E–G) Distinct functional profile of CD69⁺ cells. CD4⁺ and CD8⁺ CD69[−] and CD69⁺ memory T cells isolated from spleens and lungs were stimulated with PMA/ionomycin, and cytokine production was assessed by intracellular cytokine staining (ICS) (for IL-2, IFN- γ , and IL-17) or were stimulated with anti-CD3/CD28 beads (for IL-10), and IL-10 levels in the supernatant were assessed by BD Cytometric Bead Array. (E) Graph shows mean frequency (\pm SEM) of CD69[−] and CD69⁺ cells producing IL-2. (F) Graph indicates means \pm SEM. IL-10 production is given in picograms per milliliter. (G) Graph indicates mean frequency of CD69[−] and CD69⁺ cells producing IFN- γ (left) and IL-17A (right) \pm SEM.

n = 6 donors (spleen); ns = 10 donors (lung) for IL-2, IFN- γ , and IL-17 and 3 donors for IL-10. *p < 0.05; **p < 0.01; ***p < 0.001. Unstimulated cells had minimal cytokine production (<5%).

See also Figure S4 and Supplemental Experimental Procedures.

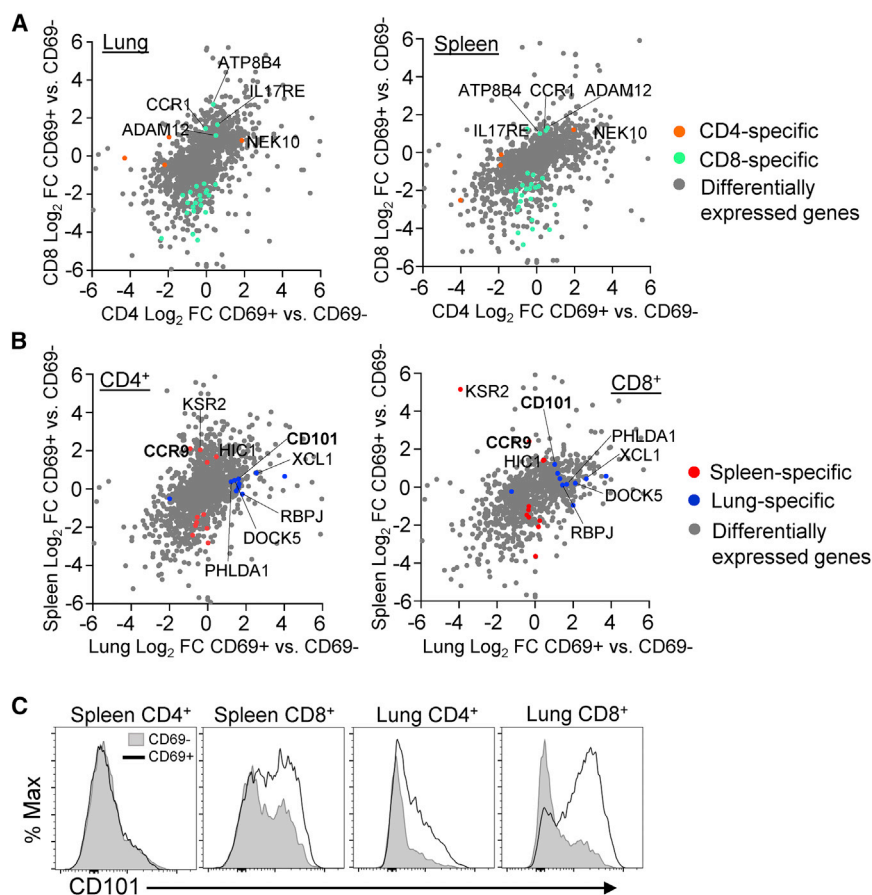


Figure 6. Lineage and Tissue-Specific Transcription and Phenotypic Profiles in Human CD69⁺ Memory T Cells

(A) Analysis of lineage-specific gene expression in CD69⁺ and CD69⁻ memory T cells. Scatterplots display log₂ fold change of CD4⁺ CD69⁺ versus CD69⁻ on the x axis and CD8⁺ subsets on the y axis from lung (left) and spleen (right). Gray dots represent genes with significant differential expression in any paired CD69⁺ versus CD69⁻ sample. Orange dots (“CD4 specific”) represent genes with significant differential expression in CD4⁺ CD69⁺ versus CD69⁻ but not in CD8⁺ samples. Green dots (“CD8 specific”) represent genes with significant differential expression in CD8⁺ CD69⁺ versus CD69⁻ but not in CD4⁺ samples.

(B) Analysis of tissue-specific genes in CD69⁺ and CD69⁻ memory T cells. Scatterplots display log₂ fold change of lung CD69⁺ versus CD69⁻ samples on the x axis and spleen samples on the y axis for CD4⁺ (left) and CD8⁺ (right) T cells, using the same strategy as in (A), with red dots denoting “spleen-specific” and blue dots denoting “lung-specific” transcripts in the paired analysis.

(C) CD101 expression in human tissues. Representative plots show CD101 expression in CD69⁺ (black outline) and CD69⁻ (shaded) cells from one individual donor. Data are representative of 15 donors.

See also Figure S5.

We assessed how multiple phenotypic properties of the core signature were distributed in diverse sites within an individual, including in intestines, mesenteric lymph nodes, tonsils, and blood in addition to lung and spleen (Figures 7C, 7D, and S6). We initially generated t-SNE plots using concatenated data from all six tissue sites, revealing phenotypically distinct TEM and TRM subsets across multiple tissues (Figure 7C). In density plots, CD4⁺ and CD8⁺ TEM cells were localized to the same region of the t-SNE, suggesting that TEM phenotypes are conserved across lineages and tissues (Figure 7C). By contrast, CD8⁺ TRM and CD4⁺ TRMs appeared at different regions within the t-SNE density plots distinct from TEM cells (Figure 7C). Notably, there was a broader range of phenotypes based on these markers within the CD4⁺ TRM subset compared with the tighter clustering of CD8⁺ TRM phenotypes, suggesting increased heterogeneity of CD4⁺ tissue memory T cells.

To compare the pattern of subset phenotypes between tissues, we assigned distinct colors to CD8⁺ TRM, CD4⁺ TRM, and TEM populations. Plotting all tissue samples on the same t-SNE reveals the localization of each cell population (Figure 7D, left), with TEM cells and CD4⁺ and CD8⁺ TRMs maintaining their distinct clustering patterns and localization in each site (Figures 7D, right, and S6). In blood, TEM cells clustered in a pattern similar to that of TEM in other tissues (Figure 7D, right), providing additional evidence that TEM cells in tissues are circulating.

Notably, CD8⁺ TRMs exhibit a focused clustering pattern in all tissues, suggesting that human TRMs represent a unique subset in multiple sites. CD4⁺ TRMs in all tissues exhibited a broader array of phenotypes, suggesting increased heterogeneity of CD4⁺ TRMs compared to CD8⁺ TRMs throughout the body.

DISCUSSION

In this study, we provide key insights into TRM biology through a comprehensive analysis of human CD4⁺ and CD8⁺ tissue memory subsets in lymphoid and mucosal tissues within and between multiple human donors. Our results establish that human tissue memory T cells fractionated based on CD69 expression exhibit a core signature of 31 genes conserved across tissues and lineages, with key homologies to the transcriptional profile of mouse TRMs. We demonstrate that human TRMs persist in multiple lymphoid, mucosal, and peripheral tissue sites; exist within both CD4⁺ and CD8⁺ lineages; and exhibit unique functional signatures, compared with circulating TEM cells, including proinflammatory and regulatory capacities and low turnover. Together, our results suggest that human TRMs are a distinct developmental subset uniquely adapted for in situ immunity.

A definitive phenotypic marker for human TRMs has not previously been defined. Transcriptional profiling has been reported for mouse CD8⁺ TRMs in which CD8⁺ memory T cells isolated from a barrier site (skin, intestine, or lung) were compared with

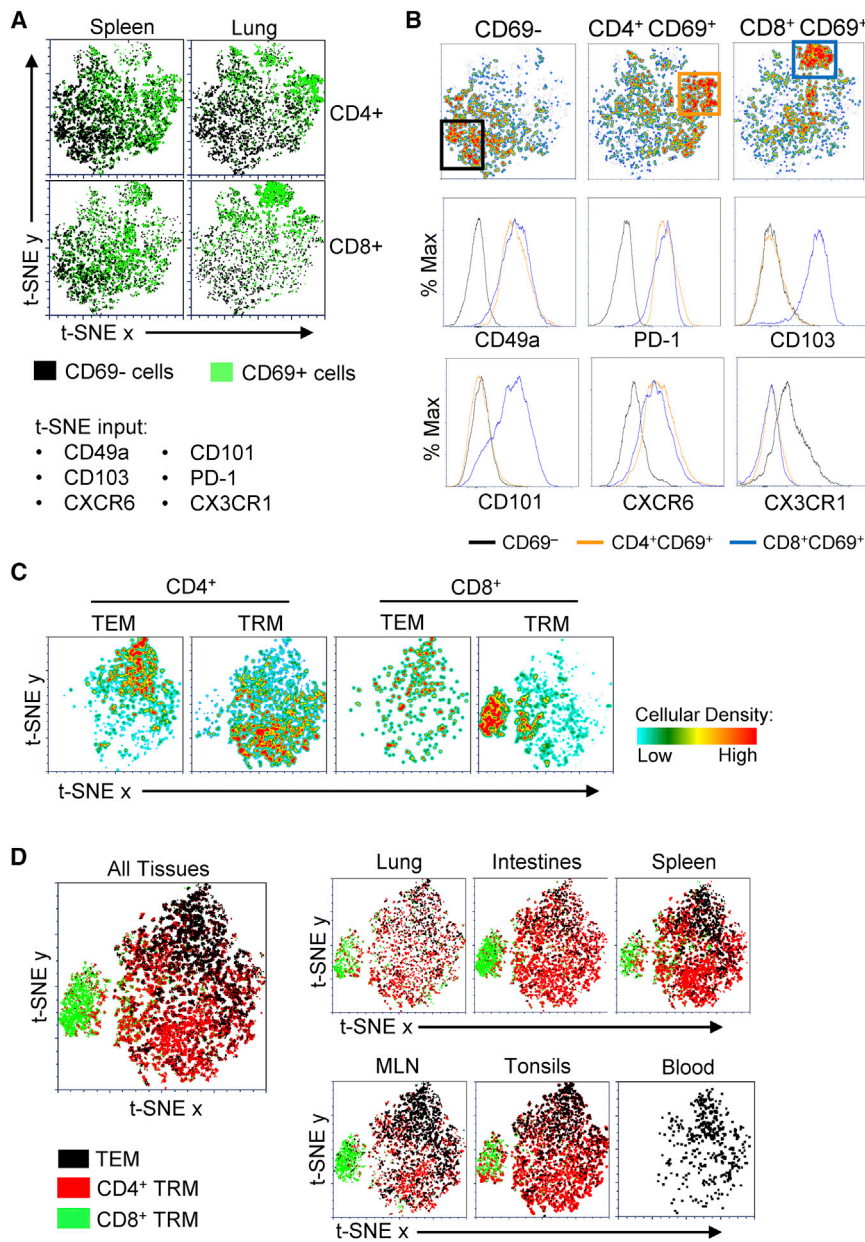


Figure 7. TRMs Are a Phenotypically Distinct Subset across Multiple Tissues

Simultaneous expression of CD49a, CD103, CD101, CXCR6, CX3CR1, PD-1, and CD69 was visualized using t-SNE analysis.

(A) CD69⁺ and CD69⁻ memory T cells are phenotypically distinct in spleen and lung. Plots show CD69⁺ memory T cells (color coded green) and CD69⁻ memory T cells (color coded black) from the spleen and lungs of an individual donor (donor 321) representative of 5 donors.

(B) Defining the phenotype of TRM and TEM clusters. Regions with high cellular density were manually gated within TEM (CD69⁻), CD4⁺ TRM (CD69⁺), and CD8⁺ TRM (CD69⁺) fractions (top row). Histograms show expression levels of CD49a, CD103, CD101, CXCR6, CX3CR1, and PD-1 within gated regions (middle and bottom rows).

(C and D) The core TRM phenotype is observed across multiple tissues. Phenotype analysis, as in (A), was performed using lung, intestine, spleen, mesenteric lymph node (MLN), tonsil, and blood samples from one representative donor (donor 332). (C) Plots show CD4⁺ (left) and CD8⁺ (right) TRM and TEM subsets from all tissues with cell number density color coded. (D) Plots shows cells from all tissues (left large plot) or each individual site (right smaller plots) color coded by cell type (CD4⁺ TRM, red; CD8⁺ TRM, green; TEM, black) of one donor representative of 4 donors. See also Figure S6.

from circulating memory T cells based on the following results: first, CD69 is the major marker that distinguishes memory T cells in diverse tissues from those in circulation for CD4⁺ and CD8⁺ T cells, while CD103 expression is limited to a subset of tissue CD8⁺ T cells. Second, CD69⁺ tissue memory T cells are a transcriptionally and phenotypically distinct subset that share core features with mouse TRMs, while human tissue CD69⁻ cells share features with circulatory blood T cells. Finally, core phenotypic markers associated the CD69⁺

T cells from spleen (Mackay et al., 2013, 2016). In human studies, CD8⁺ TRMs isolated based on CD103 expression from individual tissues (lung and skin) have been profiled in comparison to blood subsets (Cheuk et al., 2017; Hombrink et al., 2016). Here, we used an innovative and comprehensive approach to assess differences in putative circulating and resident populations within tissues by directly comparing CD69⁺ memory subsets from a lymphoid and mucosal site (spleen and lung) with the corresponding CD69⁻ subset from each tissue, as well as CD69⁻ TEM from blood for both CD4⁺ and CD8⁺ lineages. While CD103 has been used to define CD8⁺ TRMs in mice (Schenkel and Masopust, 2014) and humans (Hombrink et al., 2016), our results demonstrate that CD69 expression can delineate tissue

subset such as CD49a, PD-1, CXCR6, and CD101 delineate TRMs across multiple mucosal and lymphoid tissues.

Although we found the TRM signature to be enriched within the CD69⁺ subset of human tissue memory T cells, the role of CD69 in determining tissue residence remains unclear. In mouse models, the majority of TRMs in barrier sites express CD69; however, TRMs lacking CD69 expression have been detected (Steinert et al., 2015), and CD69⁺ cells in the thymus were shown to recirculate during homeostasis (Park et al., 2016). However, the extent of CD69 expression by tissue memory T cells appears to be a function of antigen and pathogen exposure. We consistently find higher frequencies of CD69 expression by human tissue memory T cells compared to that found in mouse models

maintained in specific pathogen free (spf) conditions, particularly in lymphoid sites (Teijaro et al., 2011; Thome et al., 2014). Interestingly, T cells in “dirty” pet store mice had significantly higher frequencies of CD69 expression by T cells in tissues that was similar to those in humans (Beura et al., 2016). In our results, we consistently see separation of transcriptional profiles between CD69⁺ and CD69[−] subsets (Figure 2), suggesting that delineation between these subsets in humans may be more defined than in mouse spf models due to the history of antigen exposure.

The core TRM gene signature identified here includes canonical genes and proteins associated with tissue residence in mice, including downregulation of S1PR1, KLF2, and CD62L; upregulation of specific adhesion molecules (CD49a and CRTAM); modulation of specific chemokine receptors (increased CXCR6 and decreased CX3CR1); and upregulation of inhibitory or regulatory molecules (PD-1, DUSP6, and IL-10). We also found TRMs to exhibit a distinct functional profile encompassing pro-inflammatory, activating, and regulatory functions conserved between diverse individuals, tissues, and lineages. We further identified a marker, CD101, with immunomodulatory function that is expressed by CD8⁺ TRMs in multiple sites and could be useful in conjunction with other markers to identify TRMs. We found phenotypic heterogeneity based on the core markers, particularly among CD4⁺ TRMs, and additional tissue heterogeneity has been reported in CyTOF profiling of human tissue T cells (Wong et al., 2016). CD103 expression by mouse intestinal TRMs (Bergsbaken and Bevan, 2015) and CD49a in human skin memory T cells (Cheuk et al., 2017) have been shown to delineate distinct functional capacities, and dissecting human TRM heterogeneity will be an important area of focus in future studies.

The dominant presence of TRMs in human tissues suggests a key protective role in situ. Our results reveal that human TRMs possess dichotomous functional capacities, not only being poised for enhanced production of IL-2 and pro-inflammatory cytokines but also producing IL-10 and exhibiting reduced proliferation and increased expression of inhibitors of T cell activation (i.e., PD-1 and CD101). This may enable the potent mobilization of immune responses in situ through pro-inflammatory cytokines but prevent excessive inflammation and cellular proliferation to limit inflammation-induced tissue damage. Moreover, the quiescent, inhibited state of TRMs as assessed by the low turnover could promote longevity and prevent inappropriate activation to non-pathogenic antigens to which many human tissues are continually exposed.

Our findings show that, in humans, TRMs exist in multiple tissue sites and within CD4⁺ and CD8⁺ T cell lineages. While TRMs have been detected in mouse lymph nodes (Schenkel et al., 2014b; Ugur et al., 2014), the majority of mouse lymphoid memory CD4⁺ and CD8⁺ T cells in mice are circulating, particularly those in the spleen. The predominance of TRM-phenotype cells in all human lymphoid tissues examined here—including spleen, lymph nodes, and tonsils—may reflect their long-term persistence over decades and/or continual pathogen exposure, consistent with a recent study identifying memory T cells specific for persistent viruses in human tonsils (Woon et al., 2016). TRM persistence in diverse sites may be due to the aggregate experience of numerous antigens over the human lifespan.

Interest in TRMs is rapidly expanding to the study of many diseases, from infection to cancer, to inflammation and autoimmunity. In humans, it is essential to identify and analyze these cells and determine whether they are functioning aberrantly in disease sites. Our study elucidates major unifying features of all tissue memory T cells in multiple healthy tissue sites within an individual. These results will serve as a valuable baseline from which to detect and study the role of tissue memory T cells in diseases and for promoting tissue immunity in vaccines as well as cell- and biologic-based immunotherapies.

EXPERIMENTAL PROCEDURES

Acquisition of Tissue from Human Organ Donors

Human tissues were obtained from deceased organ donors at the time of organ acquisition for clinical transplantation through an approved research protocol and material transfer agreement (MTA) with LiveOnNY, the organ procurement organization for the New York metropolitan area. All donors were free of chronic disease, cancer, hepatitis B, and hepatitis C, and were HIV negative. Isolation of tissues from organ donors does not qualify as “human subjects” research, as confirmed by the Columbia University Institutional Review Board (IRB). For isolation of blood from living volunteers, blood was drawn via venipuncture from consented volunteers, as approved by the Columbia University IRB. A list of donors and individuals from whom samples were obtained for this study is presented in Table S1.

Cell Isolation from Human Lymphoid and Non-lymphoid Tissues

Tissue samples were maintained in cold saline and brought to the laboratory within 2–4 hr of organ procurement. Spleen, lung, and intestinal samples were processed using enzymatic and mechanical digestion, resulting in high yields of live leukocytes, as described previously (Sathaliyawala et al., 2013; Thome et al., 2014). Lymphocytes were isolated from blood samples using centrifugation through lymphocyte separation medium (Corning) for recovery of mononuclear cells.

Flow Cytometry Analysis and Cell Sorting

For flow cytometry analysis, single-cell suspensions were stained with fluorochrome-conjugated antibodies (see Table S4 for all antibodies used in this study) in staining buffer (PBS/1% fetal bovine serum/0.1% sodium azide). Intracellular staining was performed using the Fixation/Permeabilization Solution Kit (BD Biosciences) for the detection of cytokines and Foxp3/Transcription Factor Staining Buffer (eBioscience) for the detection of transcription factors. Control samples included unstained, single fluorochrome-stained compensation beads (UltraComp eBeads; eBioscience), and fluorescence-minus-one (FMO) controls. Stained cells were acquired using the BD LSR II or BD LSRIIFortessa. Data were analyzed using FlowJo software (Tree Star) and FCS Express (De Novo Software). FCS Express software was used for generating t-SNE plots. For isolation of subsets by fluorescence-activated cell sorting, lymphocyte suspensions were enriched for T cells using the MojoSort Human CD3 T Cell Isolation Kit (BioLegend), stained for surface markers as indicated, and sorted using the BD Influx high-speed cell sorter (BD Biosciences).

Whole-Transcriptome Profiling by RNA-Seq

CD3⁺CD4⁺ and CD3⁺CD8⁺ TEM (CD45RA⁺CCR7[−]) cells were sorted into CD69⁺ and CD69[−] subsets, based on the gating strategy in Figure S1, from the spleen and lung tissue of three individual donors (D226, D233, and D250; see Table S1), and CD4⁺ and CD8⁺ TEM cells (CD45RA⁺CCR7[−]CD69[−]) were sorted from peripheral blood. RNA was isolated from cell pellets using the RNeasy Mini Kit (QIAGEN) and quantitated using an Agilent 2100 Bioanalyzer (Agilent Technologies), and library preparation and RNA-seq was performed by the Columbia Genome Center. Differential gene expression analysis was performed with EdgeR (Robinson et al., 2010), and pathway analysis was performed with Ingenuity Pathway Analysis software (IPA; QIAGEN). For GSEA with microarray data (Suárez-Fariñas et al., 2010), the absolute value of log₂

fold change between TRM and TEM cells was used to rank the genes on the x axis. For a detailed description of RNA-seq procedures and analyses, see [Supplemental Experimental Procedures](#). For a quality control (QC) summary of RNA-seq samples, see [Table S5](#).

T Cell Stimulations and Cytokine Analysis

TEM cells (CD45⁺CCR7⁺CD69⁺) and TRMs (CD45RA⁺CCR7⁺CD69⁺) were sorted from lung and spleen tissue, plated in 96-well round-bottom plates at 10⁵ cells per well in complete RPMI medium, and stimulated for 72 hr using anti-CD3/CD28/CD2 beads (T Cell Activation/Expansion Kit; Miltenyi Biotec). Supernatants from a minimum of 3 wells were pooled for each donor, and cytokine secretion was measured using the BD Cytometric Bead Array (Human Th1/Th2/Th17 Cytokine Kit). For short-term stimulations, CD4⁺ or CD8⁺ T cells from spleen and lung tissues were stimulated with Phorbol myristate acetate (PMA) (50 ng/mL) + ionomycin (1 μg/mL) for 3 hr at 37°C in the presence of BD GolgiStop. Cytokine production was assessed by intracellular staining for cytokines as described earlier.

Statistical Analysis

Descriptive statistics (percent, mean, median, and SEM) were calculated for each cell subset and tissue using Prism (GraphPad software). Significant differences in subset frequencies, ratios, geometric mean fluorescence intensity (gMFI), and density were assessed using a paired t test.

ACCESSION NUMBERS

The accession number for the RNA-seq data reported in this paper is GEO: GSE94964.

SUPPLEMENTAL INFORMATION

Supplemental Information includes Supplemental Experimental Procedures, six figures, and six tables and can be found with this article online at <http://dx.doi.org/10.1016/j.celrep.2017.08.078>.

AUTHOR CONTRIBUTIONS

B.V.K. designed experiments, processed tissues, performed flow cytometry, collected the data, and wrote the paper; W.M. analyzed RNA-seq data, made figures, and wrote the paper; D.J.C. and T.S. obtained donor tissues; S.-H.H. helped with flow cytometry experiments and analyses; X.S. performed TCR analysis; H.L. and A.L.F. coordinated tissue donation and acquisition; M.M. and R.S.G. did tissue processing and flow cytometry; T.G. did tissue processing; Y.S. planned experiments, analyzed data, and wrote the paper; D.L.F. planned experiments, coordinated tissue and data acquisition, analyzed data, and wrote the paper.

ACKNOWLEDGMENTS

This work was supported by NIH grants AI06697 and HL116136 awarded to D.L.F. Y.S. was supported by AI06697. B.V.K. was supported by T32GM007367. These studies were performed in the CCTI Flow Cytometry Core, funded in part through the S10 Shared Instrumentation grants 1S10RR027050 (LSRII), S10OD020056 (Influx), and 5P30DK063608. We wish to gratefully acknowledge the generosity of the donor families and the outstanding efforts of LiveOnNY transplant coordinators and staff for making this study possible.

Received: February 23, 2017

Revised: July 3, 2017

Accepted: August 23, 2017

Published: September 19, 2017

REFERENCES

Anderson, K.G., Mayer-Barber, K., Sung, H., Beura, L., James, B.R., Taylor, J.J., Qunaj, L., Griffith, T.S., Vezys, V., Barber, D.L., and Masopust, D.

(2014). Intravascular staining for discrimination of vascular and tissue leukocytes. *Nat. Protoc.* 9, 209–222.

Barber, D.L., Wherry, E.J., Masopust, D., Zhu, B., Allison, J.P., Sharpe, A.H., Freeman, G.J., and Ahmed, R. (2006). Restoring function in exhausted CD8 T cells during chronic viral infection. *Nature* 439, 682–687.

Bergsbaken, T., and Bevan, M.J. (2015). Proinflammatory microenvironments within the intestine regulate the differentiation of tissue-resident CD8⁺ T cells responding to infection. *Nat. Immunol.* 16, 406–414.

Bertin, S., Lozano-Ruiz, B., Bachiller, V., García-Martínez, I., Herdman, S., Zapater, P., Francés, R., Such, J., Lee, J., Raz, E., and González-Navajas, J.M. (2015). Dual-specificity phosphatase 6 regulates CD4⁺ T-cell functions and restrains spontaneous colitis in IL-10-deficient mice. *Mucosal Immunol.* 8, 505–515.

Beura, L.K., Hamilton, S.E., Bi, K., Schenkel, J.M., Odumade, O.A., Casey, K.A., Thompson, E.A., Fraser, K.A., Rosato, P.C., Filali-Mouhim, A., et al. (2016). Normalizing the environment recapitulates adult human immune traits in laboratory mice. *Nature* 532, 512–516.

Cheuk, S., Schlums, H., Gallais Sérézal, I., Martini, E., Chiang, S.C., Marquardt, N., Gibbs, A., Detlofsson, E., Introini, A., Forkel, M., et al. (2017). CD49a expression defines tissue-resident CD8⁺ T cells poised for cytotoxic function in human skin. *Immunity* 46, 287–300.

Gibbons, D.L., Abeler-Dörner, L., Raine, T., Hwang, I.Y., Jandke, A., Wencker, M., Deban, L., Rudd, C.E., Irving, P.M., Kehrl, J.H., and Hayday, A.C. (2011). Cutting edge: regulator of G protein signaling-1 selectively regulates gut T cell trafficking and colitic potential. *J. Immunol.* 187, 2067–2071.

Gordon, C.L., Miron, M., Thome, J.J., Matsuoka, N., Weiner, J., Rak, M.A., Igarashi, S., Granot, T., Lerner, H., Goodrum, F., and Farber, D.L. (2017). Tissue reservoirs of antiviral T cell immunity in persistent human CMV infection. *J. Exp. Med.* 214, 651–667.

Hombrink, P., Helbig, C., Backer, R.A., Piet, B., Oja, A.E., Stark, R., Brasser, G., Jongejans, A., Jonkers, R.E., Nota, B., et al. (2016). Programs for the persistence, vigilance and control of human CD8⁺ lung-resident memory T cells. *Nat. Immunol.* 17, 1467–1478.

Jiang, X., Clark, R.A., Liu, L., Wagers, A.J., Fuhlbrigge, R.C., and Kupper, T.S. (2012). Skin infection generates non-migratory memory CD8⁺ T(RM) cells providing global skin immunity. *Nature* 483, 227–231.

Kared, H., Martelli, S., Ng, T.P., Pender, S.L., and Larbi, A. (2016). CD57 in human natural killer cells and T-lymphocytes. *Cancer Immunol. Immunother.* 65, 441–452.

Li, B., Li, T., Wang, B., Dou, R., Zhang, J., Liu, J.S., and Liu, X.S. (2017). Ultra-sensitive detection of TCR hypervariable-region sequences in solid-tissue RNA-seq data. *Nat. Genet.* 49, 482–483.

Mackay, L.K., and Kallies, A. (2017). Transcriptional regulation of tissue-resident lymphocytes. *Trends Immunol.* 38, 94–103.

Mackay, L.K., Rahimpour, A., Ma, J.Z., Collins, N., Stock, A.T., Hafon, M.L., Vega-Ramos, J., Lauzurica, P., Mueller, S.N., Stefanovic, T., et al. (2013). The developmental pathway for CD103⁺CD8⁺ tissue-resident memory T cells of skin. *Nat. Immunol.* 14, 1294–1301.

Mackay, L.K., Braun, A., Macleod, B.L., Collins, N., Tebartz, C., Bedoui, S., Carbone, F.R., and Gebhardt, T. (2015). Cutting edge: CD69 interference with sphingosine-1-phosphate receptor function regulates peripheral T cell retention. *J. Immunol.* 194, 2059–2063.

Mackay, L.K., Minnich, M., Kragten, N.A., Liao, Y., Nota, B., Seillet, C., Zaid, A., Man, K., Preston, S., Freestone, D., et al. (2016). Hobit and Blimp1 instruct a universal transcriptional program of tissue residency in lymphocytes. *Science* 352, 459–463.

Masopust, D., Vezys, V., Marzo, A.L., and Lefrançois, L. (2001). Preferential localization of effector memory cells in nonlymphoid tissue. *Science* 297, 2413–2417.

Masopust, D., Vezys, V., Wherry, E.J., Barber, D.L., and Ahmed, R. (2006). Cutting edge: gut microenvironment promotes differentiation of a unique memory CD8 T cell population. *J. Immunol.* 176, 2079–2083.

- Matloubian, M., Lo, C.G., Cinamon, G., Lesneski, M.J., Xu, Y., Brinkmann, V., Allende, M.L., Proia, R.L., and Cyster, J.G. (2004). Lymphocyte egress from thymus and peripheral lymphoid organs is dependent on S1P receptor 1. *Nature* 427, 355–360.
- Mueller, S.N., and Mackay, L.K. (2016). Tissue-resident memory T cells: local specialists in immune defence. *Nat. Rev. Immunol.* 16, 79–89.
- Pallett, L.J., Davies, J., Colbeck, E.J., Robertson, F., Hansi, N., Easom, N.J.W., Burton, A.R., Stegmann, K.A., Schurich, A., Swadling, L., et al. (2017). IL-2(high) tissue-resident T cells in the human liver: sentinels for hepatotropic infection. *J. Exp. Med.* 214, 1567–1580.
- Park, S.L., Mackay, L.K., and Gebhardt, T. (2016). Distinct recirculation potential of CD69(+)CD103(-) and CD103(+) thymic memory CD8(+) T cells. *Immunol. Cell Biol.* 94, 975–980.
- Purwar, R., Campbell, J., Murphy, G., Richards, W.G., Clark, R.A., and Kupper, T.S. (2011). Resident memory T cells (T(RM)) are abundant in human lung: diversity, function, and antigen specificity. *PLoS ONE* 6, e16245.
- Robinson, M.D., McCarthy, D.J., and Smyth, G.K. (2010). edgeR: a Bioconductor package for differential expression analysis of digital gene expression data. *Bioinformatics* 26, 139–140.
- Sallusto, F., Lenig, D., Förster, R., Lipp, M., and Lanzavecchia, A. (1999). Two subsets of memory T lymphocytes with distinct homing potentials and effector functions. *Nature* 401, 708–712.
- Sathaliyawala, T., Kubota, M., Yudanin, N., Turner, D., Camp, P., Thome, J.J., Bickham, K.L., Lerner, H., Goldstein, M., Sykes, M., et al. (2013). Distribution and compartmentalization of human circulating and tissue-resident memory T cell subsets. *Immunity* 38, 187–197.
- Schenkel, J.M., and Masopust, D. (2014). Tissue-resident memory T cells. *Immunity* 41, 886–897.
- Schenkel, J.M., Fraser, K.A., Vezys, V., and Masopust, D. (2013). Sensing and alarm function of resident memory CD8⁺ T cells. *Nat. Immunol.* 14, 509–513.
- Schenkel, J.M., Fraser, K.A., Beura, L.K., Pauken, K.E., Vezys, V., and Masopust, D. (2014a). T cell memory. Resident memory CD8 T cells trigger protective innate and adaptive immune responses. *Science* 346, 98–101.
- Schenkel, J.M., Fraser, K.A., and Masopust, D. (2014b). Cutting edge: resident memory CD8 T cells occupy frontline niches in secondary lymphoid organs. *J. Immunol.* 192, 2961–2964.
- Shin, H., and Iwasaki, A. (2012). A vaccine strategy that protects against genital herpes by establishing local memory T cells. *Nature* 491, 463–467.
- Shiow, L.R., Rosen, D.B., Brdicková, N., Xu, Y., An, J., Lanier, L.L., Cyster, J.G., and Matloubian, M. (2006). CD69 acts downstream of interferon- α /beta to inhibit S1P1 and lymphocyte egress from lymphoid organs. *Nature* 440, 540–544.
- Skon, C.N., Lee, J.Y., Anderson, K.G., Masopust, D., Hogquist, K.A., and Jameson, S.C. (2013). Transcriptional downregulation of S1pr1 is required for the establishment of resident memory CD8⁺ T cells. *Nat. Immunol.* 14, 1285–1293.
- Soares, L.R., Tsavaler, L., Rivas, A., and Engleman, E.G. (1998). V7 (CD101) ligation inhibits TCR/CD3-induced IL-2 production by blocking Ca²⁺ flux and nuclear factor of activated T cell nuclear translocation. *J. Immunol.* 161, 209–217.
- Steinert, E.M., Schenkel, J.M., Fraser, K.A., Beura, L.K., Manlove, L.S., Igyártó, B.Z., Southern, P.J., and Masopust, D. (2015). Quantifying memory CD8 T cells reveals regionalization of immunosurveillance. *Cell* 161, 737–749.
- Suárez-Fariñas, M., Lowes, M.A., Zaba, L.C., and Krueger, J.G. (2010). Evaluation of the psoriasis transcriptome across different studies by gene set enrichment analysis (GSEA). *PLoS ONE* 5, e10247.
- Subramanian, A., Tamayo, P., Mootha, V.K., Mukherjee, S., Ebert, B.L., Gillette, M.A., Paulovich, A., Pomeroy, S.L., Golub, T.R., Lander, E.S., and Mesirov, J.P. (2005). Gene set enrichment analysis: a knowledge-based approach for interpreting genome-wide expression profiles. *Proc. Natl. Acad. Sci. USA* 102, 15545–15550.
- Teijaro, J.R., Turner, D., Pham, Q., Wherry, E.J., Lefrançois, L., and Farber, D.L. (2011). Cutting edge: Tissue-retentive lung memory CD4 T cells mediate optimal protection to respiratory virus infection. *J. Immunol.* 187, 5510–5514.
- Thom, J.T., Weber, T.C., Walton, S.M., Torti, N., and Oxenius, A. (2015). The salivary gland acts as a sink for tissue-resident memory CD8(+) T cells, facilitating protection from local cytomegalovirus infection. *Cell Rep.* 13, 1125–1136.
- Thome, J.J., and Farber, D.L. (2015). Emerging concepts in tissue-resident T cells: lessons from humans. *Trends Immunol.* 36, 428–435.
- Thome, J.J.C., Yudanin, N., Ohmura, Y., Kubota, M., Grinshpun, B., Sathaliyawala, T., Kato, T., Lerner, H., Shen, Y., and Farber, D.L. (2014). Spatial map of human T cell compartmentalization and maintenance over decades of life. *Cell* 159, 814–828.
- Thome, J.J., Bickham, K.L., Ohmura, Y., Kubota, M., Matsuoka, N., Gordon, C., Granot, T., Griesemer, A., Lerner, H., Kato, T., and Farber, D.L. (2016a). Early-life compartmentalization of human T cell differentiation and regulatory function in mucosal and lymphoid tissues. *Nat. Med.* 22, 72–77.
- Thome, J.J., Grinshpun, B., Kumar, B.V., Kubota, M., Ohmura, Y., Lerner, H., Sempowski, G.D., Shen, Y., and Farber, D.L. (2016b). Longterm maintenance of human naive T cells through in situ homeostasis in lymphoid tissue sites. *Sci. Immunol.* 1, eaah6506.
- Turner, D.L., Bickham, K.L., Thome, J.J., Kim, C.Y., D'Ovidio, F., Wherry, E.J., and Farber, D.L. (2014). Lung niches for the generation and maintenance of tissue-resident memory T cells. *Mucosal Immunol.* 7, 501–510.
- Ugur, M., Schulz, O., Menon, M.B., Krueger, A., and Pabst, O. (2014). Resident CD4⁺ T cells accumulate in lymphoid organs after prolonged antigen exposure. *Nat. Commun.* 5, 4821.
- van der Matten, L., and Hinton, G. (2008). Visualizing data using t-SNE. *J. Mach. Learn. Res.* 9, 2579–2605.
- Wakim, L.M., Woodward-Davis, A., Liu, R., Hu, Y., Villadangos, J., Smyth, G., and Bevan, M.J. (2012). The molecular signature of tissue resident memory CD8 T cells isolated from the brain. *J. Immunol.* 189, 3462–3471.
- Watanabe, R., Gehad, A., Yang, C., Scott, L.L., Teague, J.E., Schlapbach, C., Elco, C.P., Huang, V., Matos, T.R., Kupper, T.S., and Clark, R.A. (2015). Human skin is protected by four functionally and phenotypically discrete populations of resident and recirculating memory T cells. *Sci. Transl. Med.* 7, 279ra39.
- Wong, M.T., Ong, D.E., Lim, F.S., Teng, K.W., McGovern, N., Narayanan, S., Ho, W.Q., Cerny, D., Tan, H.K., Anicete, R., et al. (2016). A high-dimensional atlas of human T cell diversity reveals tissue-specific trafficking and cytokine signatures. *Immunity* 45, 442–456.
- Woon, H.G., Braun, A., Li, J., Smith, C., Edwards, J., Sierro, F., Feng, C.G., Khanna, R., Elliot, M., Bell, A., et al. (2016). Compartmentalization of total and virus-specific tissue-resident memory CD8⁺ T cells in human lymphoid organs. *PLoS Pathog.* 12, e1005799.
- Zens, K.D., Chen, J.-K., and Farber, D.L. (2016). Vaccine-generated lung tissue-resident memory T cells provide heterosubtypic protection to influenza infection. *JCI Insight* 1, e85832.